The EMBO Journal (2007) 26, 41–52 | © 2007 European Molecular Biology Organization | All Rights Reserved 0261-4189/07
www.embojournal.org

THE EMBO JOURNAL

Moesin regulates stable microtubule formation and limits retroviral infection in cultured cells

Mojgan H Naghavi[1,4], Susana Valente[1], Theodora Hatziioannou[2], Kenia de los Santos[1], Ying Wen[3], Christina Mott[1], Gregg G Gundersen[3] and Stephen P Goff[1,*]

[1]Department of Biochemistry and Molecular Biophysics, Howard Hughes Medical Institute, College of Physicians and Surgeons, Columbia University, New York, NY, USA, [2]Aaron Diamond AIDS Research Center, New York, NY, USA and [3]Department of Anatomy and Cell Biology, Columbia University, New York, NY, USA

In a functional screen of mammalian complementary DNA libraries, we identified moesin as a novel gene whose overexpression blocks infection by murine leukemia viruses and human immunodeficiency virus type 1 in human and rodent lines, before the initiation of reverse transcription. Knockdown of moesin by RNA interference resulted in enhanced infection, suggesting that even the endogenous basal levels of moesin in rat fibroblasts are sufficient to limit virus infection. Moesin acts as a cross-linker between plasma membrane and actin filaments, as well as a signal transducer in responses involving cytoskeletal remodeling. Moesin overexpression was found to downregulate the formation of stable microtubules, whereas knockdown of moesin increased stable microtubule formation. A virus-resistant mutant cell line also displayed decreased stable microtubule levels, and virus-sensitive revertants recovered from the mutant line showed restoration of the stable microtubules, suggesting that these cytoskeletal networks play an important role in early post-entry events in the retroviral lifecycle. Together, these results suggest that moesin negatively regulates stable microtubule networks and is a natural determinant of cellular sensitivity to retroviral infection.

The EMBO Journal (2007) **26,** 41–52. doi:10.1038/sj.emboj.7601475; Published online 14 December 2006
Subject Categories: cell & tissue architecture; microbiology & pathogens
Keywords: HIV-1; moesin; retroviruses; stable microtubules; viral block

*Corresponding author. Department of Biochemistry and Molecular Biophysics, Howard Hughes Medical Institute, Columbia University, HHSC 1310, 701 West 168th Street, New York, NY 10032, USA.
Tel.: +1 212 305 7956; Fax: +1 212 305 5106;
E-mail: goff@cancercenter.columbia.edu
[4]Present address: Center for Research in Infectious Diseases, Conway Institute of Molecular and Biomedical Research, University College Dublin, Belfield, Dublin 4, Ireland

Received: 11 July 2006; accepted: 6 November 2006; published online: 14 December 2006

Introduction

Understanding the mechanisms by which cellular factors block retroviral infection can provide invaluable insights into host–virus interactions and highlight possible strategies for therapeutic intervention. Recently, functional screening of complementary DNA (cDNA) expression libraries for host genes that conferred virus resistance resulted in the isolation of two resistance factors: zinc-finger antiviral protein, which specifically inhibits the accumulation of murine leukemia virus (MLV) (Gao *et al*, 2002) and many alphavirus (Bick *et al*, 2003) mRNAs in the cytoplasm, and the tripartite interaction motif 5α (TRIM5α), which blocks incoming virus at an early post-entry step before reverse transcription (Stremlau *et al*, 2004). In addition, other screens have identified dominant interfering versions of inherently positive genes, such as Tsg101 (Garrus *et al*, 2001; von Schwedler *et al*, 2003) and the Nedd4-like ubiquitin ligases (Kikonyogo *et al*, 2001; Yasuda *et al*, 2002) required for the budding of several enveloped viruses. Both sets of genes have provided important insights into novel aspects of viral replication.

The identification of additional factors that affect virus replication will add to our understanding of virus–host interactions. Here, we report the identification of a novel antiretroviral factor, moesin, from a screen of a cDNA library from the virus-resistant cell line R4-7 (Gao and Goff, 1999). Moesin overexpression blocks infection by both MLV and HIV-1 viruses before the initiation of reverse transcription, and moesin knockdown enhances infection. A cytoskeletal regulatory protein that colocalizes with actin filaments at cell-surface structures, moesin crosslinks actin in the cortical layer, and can thereby control cell shape and movement. We show that moesin negatively regulates stable microtubule formation and propose a novel role for stable microtubules in the post-entry movement of viral particles. The ability of endogenous levels of moesin to limit retroviral replication suggests that moesin may be a natural determinant of cellular sensitivity to infection.

Results

To identify factors that could block retroviral infection, a library of expressed cDNAs from the virus-resistant cell line, R4-7 (Gao and Goff, 1999) was constructed in the pBabe-HAZ expression vector (Gao *et al*, 2002). The complexity of the library was 1.5×10^6, with inserts ranging from 0.8 to 2.5 kb. An aliquot of the cDNA library was used to generate MLV-based transducing viruses, which were applied to thymidine kinase-negative (TK−) Rat2 cells (Supplementary Figure S1). A pool of the transduced cells was then challenged by repeated infection with an HIV-1 vector expressing the TK gene (Gao *et al*, 2002). Selection of 1×10^4 transduced lines in trifluorothymidine resulted in the isolation of 31 TK-negative clones as candidate virus-resistant cells. The cDNA inserts in 25 of the clones were recovered from the genomic

DNA by PCR amplification and sequenced (Supplementary Table S1). Notably, 11 out of 25 DNA sequences encoded the N-terminal 342 amino acids of moesin fused to the zeocin resistance gene, termed N-Msn-zeo. Tests of the level of expression of moesin in the virus-resistant R4-7 line showed no significant change as compared to the wild-type (wt) Rat2 cells (Figure 1E). Examination of multiple moesin cDNAs isolated from R4-7 (Gao and Goff, 1999) revealed no

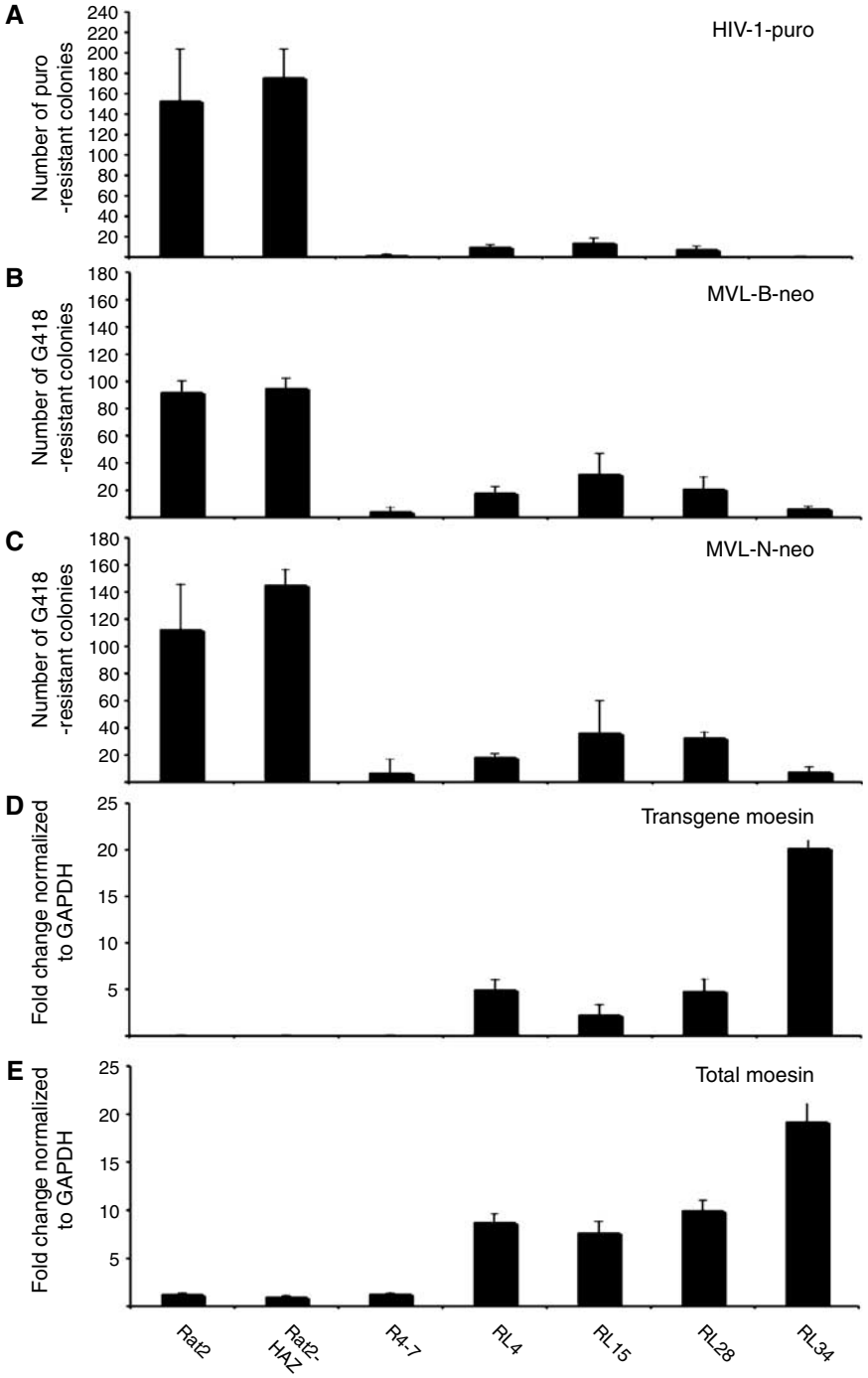

Figure 1 Expression of the N-terminus of moesin confers resistance to retroviral infection. (**A–C**) Overexpression of N-Msn-zeo in Rat2 cells isolated from the library screen blocks retrovirus infection. Wt Rat2 fibroblasts, Rat2; Rat2 cells containing empty pBabe-HAZ vector, Rat2-HAZ; the control virus-resistant R4-7 cells; or the Rat2 lines containing pBabe-HAZ vector expressing N-Msn-zeo, RL-, 4, 15, 28 and 34, were incubated with various amounts of HIV-1-puro (A), MLV-B-neo (B) and MLV-N-neo (C) viruses. Cells were selected in medium containing puromycin (A; HIV-1) or G418 (B and C; neo-viruses) and the number of transduced colonies were counted after 8–12 days. Similar results were obtained in at least three independent experiments. (**D, E**) Quantitative RT-PCR showing the level of moesin expression in Rat2 cells. Cytoplasmic RNA prepared from the same cell lines used in the transduction assay (A–C) was converted to ds cDNA and used as template for QRT-PCR. Primers unique to each cDNA sequence were used to distinguish transgene (D) and total (E) moesin transcripts. The fold-change ratios between the Rat2 mutant lines and the control empty vector Rat2-HAZ line are median copy numbers normalized to GAPDH copy numbers obtained in duplicate from two independent RNA preparations.

significant nucleotide polymorphisms relative to the parental Rat2 cells (data not shown). Thus, although it was the source of the moesin cDNA, overexpression or mutation(s) of the moesin gene was not responsible for the virus-resistant phenotype of the R4-7 line.

The retroviral resistance of four of the N-Msn-zeo-expressing clones was confirmed by challenging with a number of genetically marked retroviruses, followed by growth in selective medium and counting of drug-resistant colonies (Naghavi *et al*, 2005). All clones showed a potent resistance to infection by HIV-1-puro (HIV-based viral vector carrying the puromycin resistance marker), with titers reduced by factors ranging from 20- to 600-fold (Figure 1A), as well as a lesser but significant resistance to MLV-B-neo and MLV-N-neo (B-tropic or N-tropic MLV-based viral vectors carrying the neomycin resistance marker) viruses (Figure 1B and C, respectively). As seen previously, the virus-resistant R4-7 line from which the cDNA library was derived showed a similarly high level of resistance to retroviral challenge (Gao and Goff, 1999). To determine whether the levels of retroviral resistance detected in the N-Msn-zeo-expressing cells correlated with the expression levels of N-Msn-zeo transcripts in these lines, we used a quantitative real-time PCR assay (QRT-PCR) (Naghavi *et al*, 2005). The transgene moesin was distinguished from the total (endogenous and transgene) moesin transcripts by using a primer unique to the vector sequence. All N-Msn-zeo-expressing lines showed a pattern of expression for transgene (Figure 1D) and total (Figure 1E) moesin that correlated closely with the levels of resistance to both HIV-1 (Figure 1A) and MLV (Figure 1B and C) infection. N-Msn-zeo was also found to block HIV-1-puro infection in both HeLa (data not shown) and 293A cells (Figure 2C and D). Thus, N-Msn-zeo blocks retroviral infection in both rat and human lines.

To confirm that N-Msn-zeo cDNA was responsible for the resistance in these lines, the proviral DNA-expressing moesin was excised at the flanking Lox-P sites following transfection of resistant clones with a Cre recombinase-expressing construct (Gao *et al*, 2002). Excision of the cDNA in four clones (Supplementary Figure S2C) significantly restored

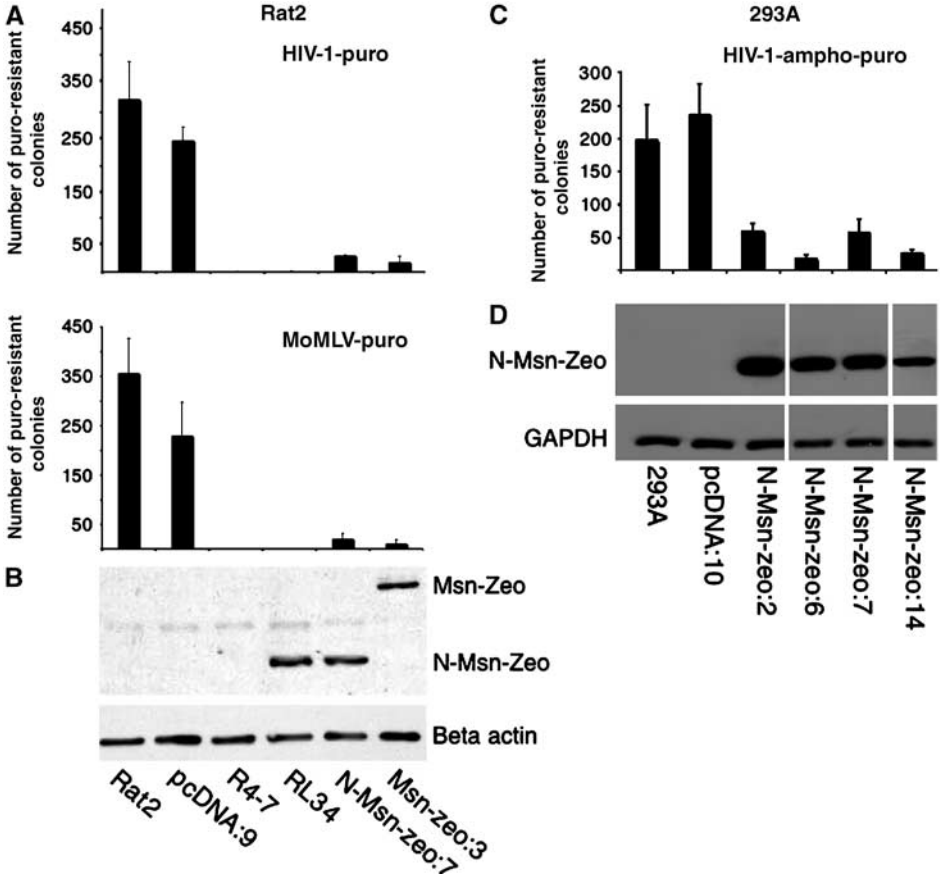

Figure 2 Zeocin-fused moesin can confer resistance to retroviruses in both Rat2 and human lines. (**A**) Rat2 cells stably transduced with the empty vector (pcDNA:9) or stably expressing zeocin-tagged full-length (Msn-zeo:3) or C-terminally truncated (N-Msn-zeo:7) moesin were incubated with various amounts of HIV-1-puro or MoMLV-puro. Wt Rat2 cells, Rat2; the control virus-resistant line, R4-7; one of the N-Msn-zeo-expressing lines isolated from the library screening, RL34. Cells were plated in medium containing puromycin and the number of transduced colonies was counted after 10 days. Similar results were obtained in at least three independent experiments. Full-length or C-terminally truncated zeocin-tagged moesin (indicated as Msn-zeo and N-Msn-zeo, respectively) expression was detected in the same lines using immunoblotting with anti-zeocin antibodies (**B**, upper panel). Loading of equal amounts of protein was confirmed using β-actin antibodies (B, lower panel). (**C**) wt 293A cells, 293A cells stably transduced with the control empty vector (pcDNA:10) or cells stably expressing C-terminally truncated moesin fused to zeocin (N-Msn-zeo:2, 6, 7 and 14) were incubated with various amount of HIV-1-amhpo-puro and selected in puromycin as described for Rat2 cells. (**D**) Upper panel. C-terminally truncated zeocin-tagged moesin expression was detected in the same lines using immunoblotting with anti-zeocin antibodies. D, Lower panel: Loading of equal amounts of protein was confirmed using GAPDH antibodies.

their susceptibility to infection by both MoMLV-puro (Moloney) and HIV-1-puro (Supplementary Figure S2A and B, respectively), whereas clones that retained the cDNA remained resistant, confirming that the continued expression of N-Msn-zeo cDNA was required and responsible for the resistance phenotype of these lines. To analyze whether the C-terminal truncation or the zeocin fusion at the 3′ end of N-Msn-zeo cDNA was responsible for the resistance phenotype, full-length or C-terminally truncated moesin cDNAs, with or without the zeocin fusion, were recloned into the mammalian expression vector pcDNA3.1$^+$ and introduced into Rat2 fibroblasts. Stable drug-resistant cell lines were isolated and tested for resistance. All four variants of moesin conferred resistance to both HIV-1-puro (Figure 2A and Supplementary Figure S3A) and MoMLV-puro (Figure 2B and Supplementary Figure S3B), relative to control Rat2 cells or the empty vector pcDNA:9 line. In addition, these clones also inhibited replication of wt Moloney virus, as measured by the rate of appearance of reverse transcriptase (RT) in culture media of infected cells (Figure 3). Expression of zeocin-tagged moesin protein was confirmed using immunoblotting with anti-zeocin antibodies (Figure 2B), whereas untagged moesin expression levels were determined by QRT-PCR measurement of mRNAs (Naghavi *et al*, 2005) (Supplementary Figure S3C) as suitable antibodies were not available. As expected, no transgene expression of moesin was detected in the wt Rat2, the empty pcDNA:9 vector or the R4-7 line (Figure 2B and Supplementary Figure S3C). In conclusion, the data indicated that the N-terminal domain of moesin was sufficient to induce a potent resistance to infection by both genetically marked and wt retroviruses.

To test whether the endogenous levels of moesin also affect virus susceptibility, RNA interference (RNAi) was used to reduce moesin levels in rat cells and the consequences were assessed by challenging the cultures by infection with genetically marked retroviruses. wt Rat2 or mutant R4-7 cells were treated with two independent short-interfering RNA (siRNA) duplexes (Ambion) or control duplexes. Moesin-specific RNAi duplexes induced an approximately three- to five-fold increase in susceptibility of both Rat2 and R4-7 lines to both MoMLV-puro and HIV-1-puro infection, whereas a nonspecific siRNA duplex targeted to GFP had no effect (Figure 4A). The partial increase in susceptibility correlated with a three- to four-fold knockdown of moesin transcripts in these cells (Figure 4B). The results suggest that the endogenous basal levels of moesin in Rat2 cells are sufficient to limit virus infection, and that moesin is a natural determinant of cellular sensitivity to retroviral infection.

To determine the step in the viral life cycle that was blocked by moesin, viral DNA synthesis was examined after acute infection of N-Msn-zeo-expressing lines with ecotropic MLV-GFP (Naghavi *et al*, 2005). The resistant cells produced only very low levels of linear viral DNA (GFP; Figure 5A), minus-strand strong stop DNA (MSS; Figure 5B), plus-strand DNA (PS; Figure 5C) and circular DNA (long terminal repeat (LTR)–LTR; Figure 5D), suggesting a block before initiation of reverse transcription. Using HIV-1 cores that contain a Vpr-β-lactamase fusion protein (Cavrois *et al*, 2002) to monitor viral penetration into the cytosol, we demonstrated normal entry of virus in both R4-7 and the moesin-overexpressing line RL4 (Supplementary Figure S4A). It must be noted that this assay required the use of a high multiplicity of infection

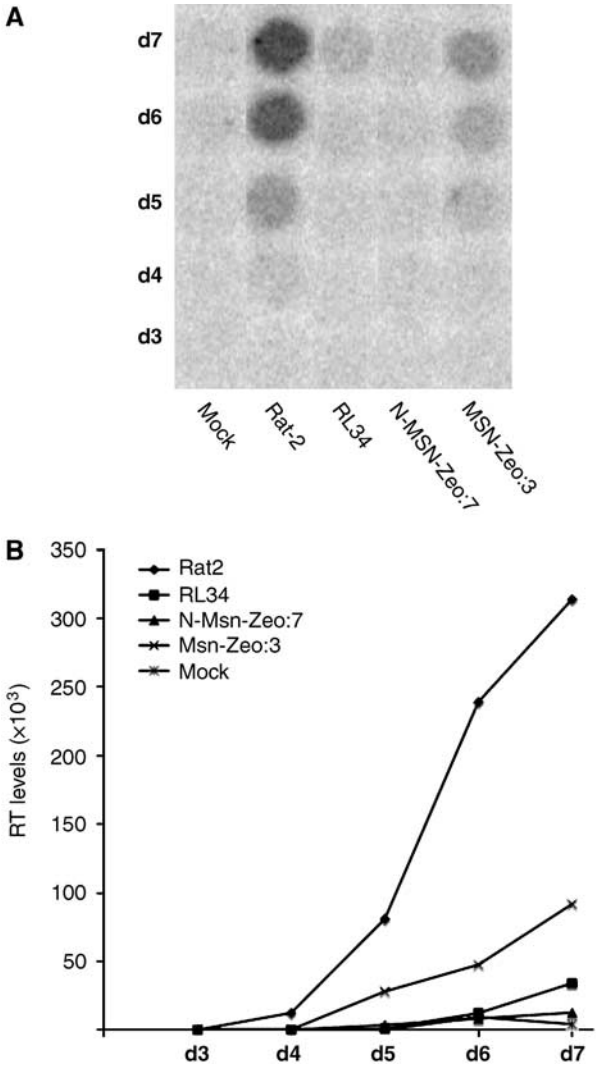

Figure 3 Assembly and release of Moloney virions measured by reverse transcriptase (RT) assay. (**A**) Spots indicate the amount of labeled nucleotide incorporated in an exogenous RT assay on a homopolymer template by virion-associated RT. Equal amounts of virus were used to infect naïve Rat2, the N-Msn-zeo line isolated from the library screen (RL34), the stably expressing zeocin-tagged C-terminally truncated (N-Msn-zeo:7) or the full-length (Msn-zeo:3) moesin lines. Culture supernatants were collected on successive days as indicated, and virus production was monitored by RT assay. Mock, no virus was applied. (**B**) Quantification of viral replication assay shown in (A). Dot intensities were normalized against uninfected cell samples.

by the reporter virus, which saturates the viral block (Supplementary Figure S4B). However, taken together with the fact that these lines block the replication of a number of retroviruses pseudotyped with different envelope glycoproteins—vesicular stomatitis virus (VSV-G) (Figures 1–3 and Supplementary Figures S2 and S3), ecotropic (Figure 5) or amphotropic envelopes (Supplementary Figure S5)—that enter the cell by various means, these preliminary findings suggest that the block to infection occurs after viral fusion but before reverse transcription, the same step at which retrovirus replication is blocked in the R4-7 line (Gao and Goff, 1999).

We then tested whether the retrovirus-resistant R4-7 line had a general defect in sorting or trafficking by visualizing

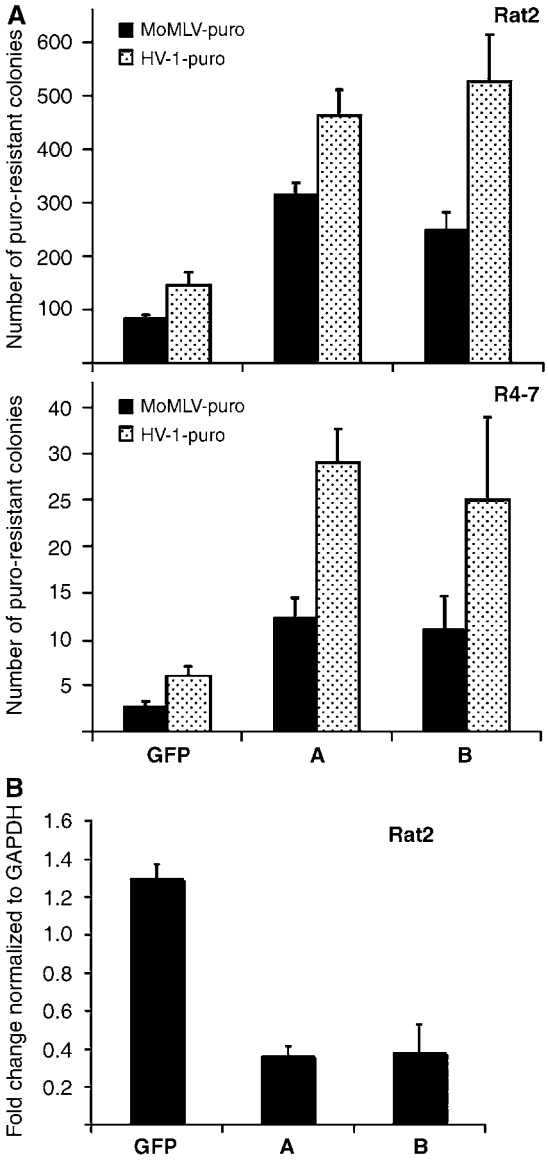

Figure 4 RNAi to moesin increases the virus susceptibility of both wt Rat2 cells and the mutant R4-7 line. (**A**) The wt Rat2 cells or mutant R4-7 cells were transfected with two independent short-interfering RNAs (as indicated in A, B) on two consecutive days with equal amounts of RNA duplexes and subsequently seeded and infected with various amounts of MoMLV-puro or HIV-1-puro. Cells were selected in medium containing puromycin and the number of transduced colonies was counted after 10 days. The nonspecific GFP duplex was included as a negative control. Similar results were obtained in at least three independent experiments. (**B**) Quantitative RT–PCR showing the level of endogenous moesin expression in Rat2 cells transfected with nonspecific (GFP) or moesin-specific (A, B) siRNA duplexes.

endocytosed transferrin in these cells. Target cells were incubated with fluorescently labeled transferrin at 4°C, shifted to 37°C and fixed at various time points thereafter. As expected, within 10 min after shifting to 37°C, the majority of the labeled transferrin in Rat2 cells was concentrated in a discrete spot (Figure 6A), most likely corresponding to the recycling endosome. In contrast, in R4-7 cells, this discrete staining was not observed and the transferrin appeared as a diffuse cytoplasmic stain (Figure 6A). This defect in transferrin trafficking to the endosome was specific to R4-7 cells, as another previously described R3-2 mutant cell line, resistant to infection at a later stage in the viral life cycle (Gao and Goff, 1999), exhibited transferrin staining that was similar to, although less intense than, the control Rat2 cells (Figure 6A). To further confirm that the change in staining is indeed a sorting/trafficking defect, the uptake of transferrin was quantified in Rat2, R4-7 as well as in the moesin-overexpressing lines (RL34, N-Msn:5 and Msn:6), as previously described (Hinrichsen *et al*, 2003). Serum-starved cells were incubated with biotin-labeled transferrin (Molecular Probes) on ice for 1 h and the bound transferrin was allowed to internalize for various lengths of time at 37°C (2, 5 and 8 min to avoid any recycling). Internalized biotinylated transferrin was quantitated by Western blotting using NeutraAvidin conjugated to horseradish peroxidase (Molecular Probes). There was no significant change in the levels or rate of transferrin uptake in all lines (Figure 6B), suggesting that there was a specific defect in endosomal sorting rather than endocytosis in the virus-resistant lines.

It has been reported that transferrin trafficking is linked specifically to a subset of detyrosinated microtubules lacking the carboxy-terminal tyrosine (Lin *et al*, 2002). This subset is more stable than the majority (90%) of microtubules (Westermann and Weber, 2003). The availability of antibodies specific for detyrosinated tubulin (termed Glu-MTs) as well as for tyrosinated tubulin (Tyr-MTs) (Gundersen *et al*, 1984) allowed a comparison of the different microtubule networks in both mutant and wt cells. Rat2 or virus-resistant cells were grown on coverslips and stained with the two different tubulin antibodies. Surprisingly, both the mutant R4-7 cells and the moesin-overexpressing RL34 line showed significantly lower levels of stable Glu-MTs (22 and 52% of cells staining positive, respectively) compared with control Rat2 cells (79% positive) (Figure 7). This defect in the virus-resistant lines was specific for stable microtubules, as staining for tyrosinated microtubules revealed levels and patterns of expression similar to those seen in Rat2 cells (Figure 7). Overexpression of these various moesin fragments did not have any significant effect on cell parameters such as shape, size or doubling time (19 h for wt Rat2 and 20–21 h for the moesin-overexpressing lines; data not shown). In addition, knockdown of moesin using two specific siRNA duplexes (Msn-A and Msn-B) but not with a nonspecific siRNA duplex targeting GFP sequences (Figure 8A) increased the proportion of Glu-MT-positive cells in both Rat2 (1.2-fold) and R4-7 (three-fold) cells, correlating with the increased virus sensitivity of moesin siRNA-treated cells (Figure 4A). Again, the levels of Tyr-MTs were normal in all of these lines (Figure 8B).

Previous findings have demonstrated that the virus resistance phenotype of the R4-7 line is reversed by the expression of two non-coding RNAs (Gao and Goff, 2004). The mechanism by which these RNAs restore the susceptibility to infection is unknown. However, immunofluorescent staining demonstrates that stable microtubule formation is restored in both R4-7 suppressor clones pC1-2 and pB1-11, expressing these RNAs (Figure 9A), in contrast to the original virus-resistant R4-7 cells and the empty vector pControl-transfected R4-7. As expected, the R3-2 line, which showed normal transferrin trafficking, displayed normal levels of Glu-MTs (Figure 9A). Again, tyrosinated microtubule formation was unchanged in each of the lines examined (Figure 9B).

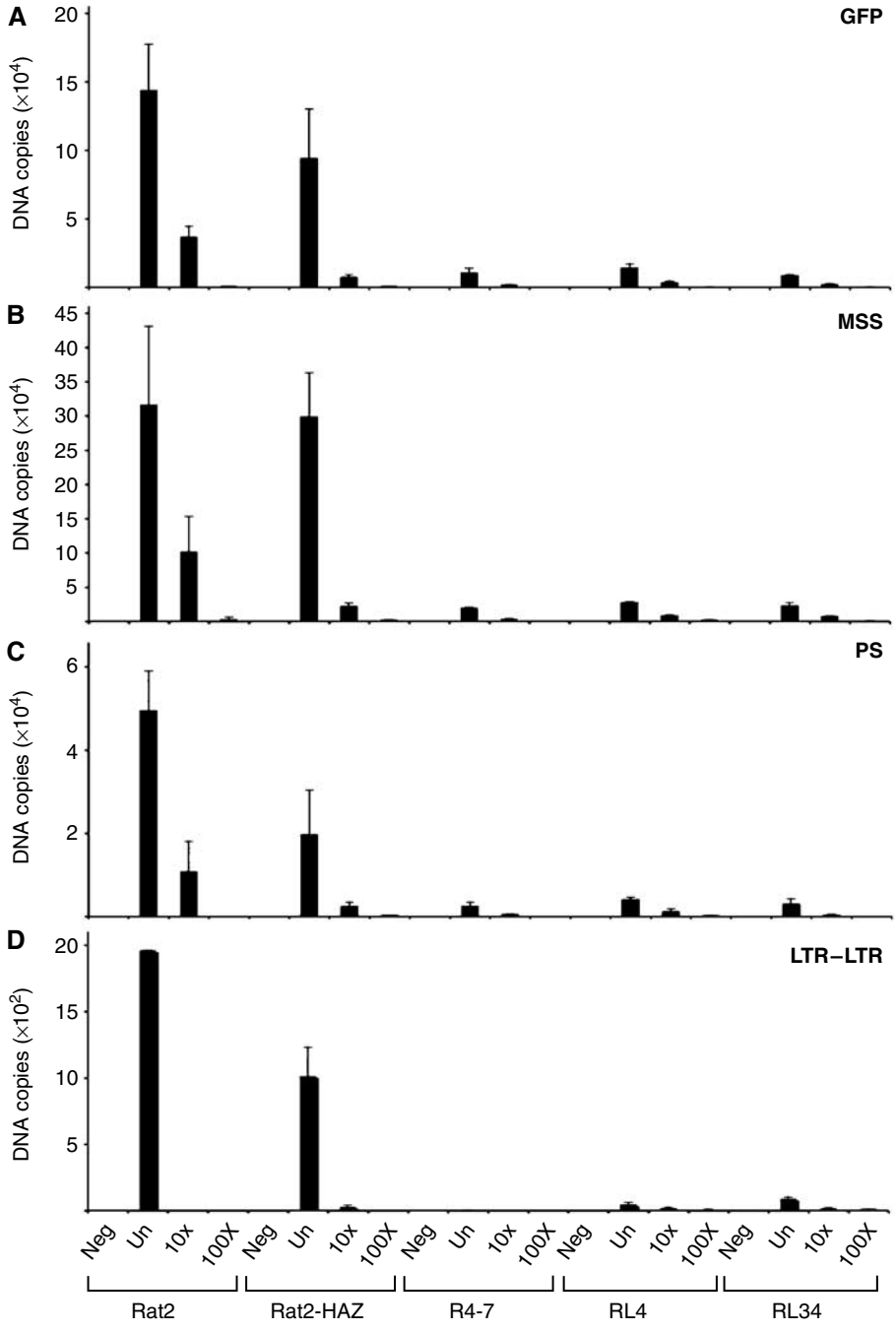

Figure 5 Analysis of the block to virus infection using quantitative RT-PCR. Wt Rat2 cells, the control empty vector Rat2-HAZ line, the control virus-resistant R4-7 line and two of the N-Msn-zeo lines isolated from the screen (RL4 and RL34) were infected with either undiluted (un) or 10-fold serially diluted ($10\times$, $100\times$) ecotropic MLV-GFP. Uninfected cells were included as a negative control (indicated as neg) for each sample. Total DNA was isolated at 24 h after infection and the amount of viral DNA synthesized in the infected cells was measured by QRT-PCR. Using primers specific to GFP sequences, minus-strand strong stop (MSS) DNA, plus-strand DNA (PS) or LTR–LTR junction, the amount of total linear viral DNA (**A**), MSS DNA (**B**), PS DNA (**C**) or circular viral DNA in the nucleus (**D**) was determined. Each DNA sample was assayed in duplicate at a minimum of three different time points.

In agreement with this observation, the fraction Glu-MT-positive cells in an RL4-cre clone, which no longer contained the moesin cDNA and had restored virus sensitivity, RL4-cre:1, was comparable to that of the control empty vector Rat-HAZ (79 and 78%, respectively) (Supplementary Figure S6). As expected, in the virus-resistant clone RL4-cre:10, in which cre did not excise the cDNA, the fraction of Glu-MT-positive cells was similar to that in the moesin-over-expressing line RL34 (52%). These results provide multiple independent lines of evidence to suggest that the loss of stable microtubules in the R4-7 line as well as in the moesin-overexpressing lines is linked to virus resistance. In summary, these findings strongly suggest a role for stable microtubules in the early stages of the retroviral life cycle and a role for moesin in negatively regulating stable microtubule networks and retroviral susceptibility.

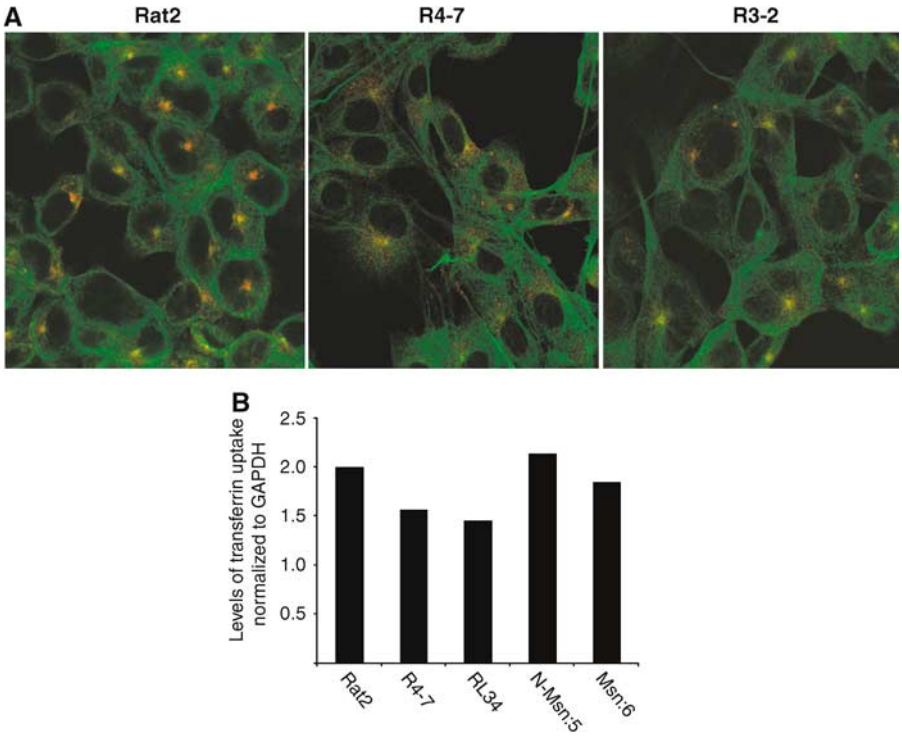

Figure 6 Trafficking and uptake of endocytosed transferrin in retrovirus-resistant and-sensitive cell lines. (**A**) Trafficking of endocytosed transferrin. Wt Rat2 cells or the virus-resistant lines R4-7 and R3-2 were incubated with fluorescently labeled transferrin at 4°C, shifted to 37°C and fixed after 10 min. Cells were then permeabilized and microtubule networks visualized using anti-tubulin antibodies, followed by detection with FITC-labeled secondary antibodies. Images were taken as described in Materials and methods. Red indicates transferrin and green indicates total microtubules. (**B**) Quantification of transferrin uptake. Serum-starved wt Rat2 cells, R4-7 or the moesin-overexpressing lines (RL34, N-Msn:5 and Msn:6) were incubated with biotin-labeled transferrin on ice for 1 h. Bound transferrin was allowed to internalize for various lengths of time at 37°C (2, 5 and 8 min) and further quantified by Western blotting using NeutraAvidin conjugated to horseradish peroxidase. The average rate of transferrin uptake normalized to the average rate of GAPDH for each line is presented.

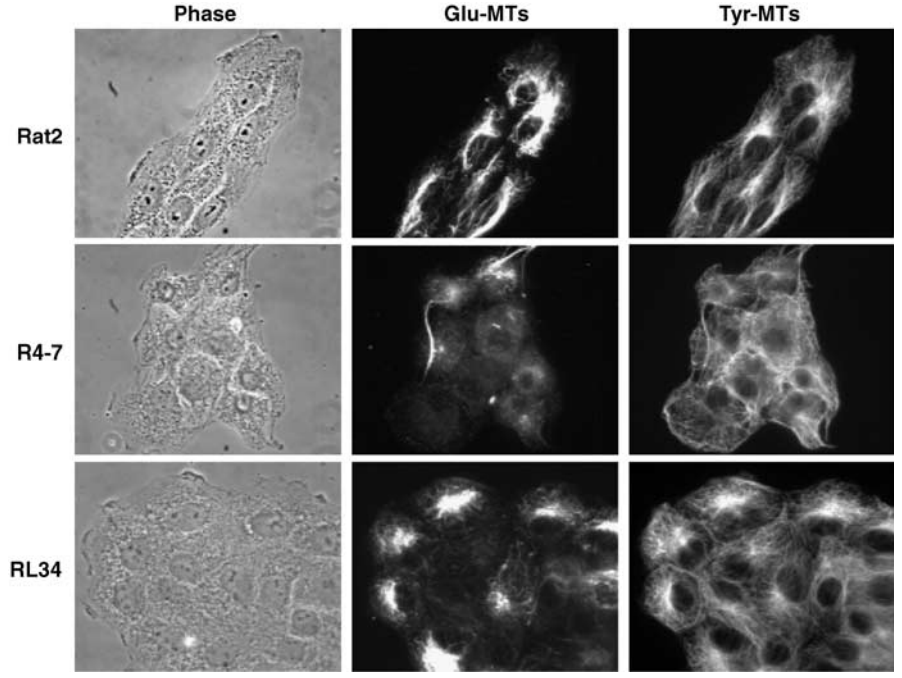

Figure 7 Virus-resistant lines display decreased stable microtubule formation. Wt Rat2 cells, the virus-resistant R4-7 cells and the moesin-overexpressing line RL34 were fixed, stained with a rabbit polyclonal antibody for stable Glu-MTs and a rat mAb for dynamic Tyr-MTs followed by incubation with fluorescently labeled secondary antibodies. Images were taken as described in Materials and methods.

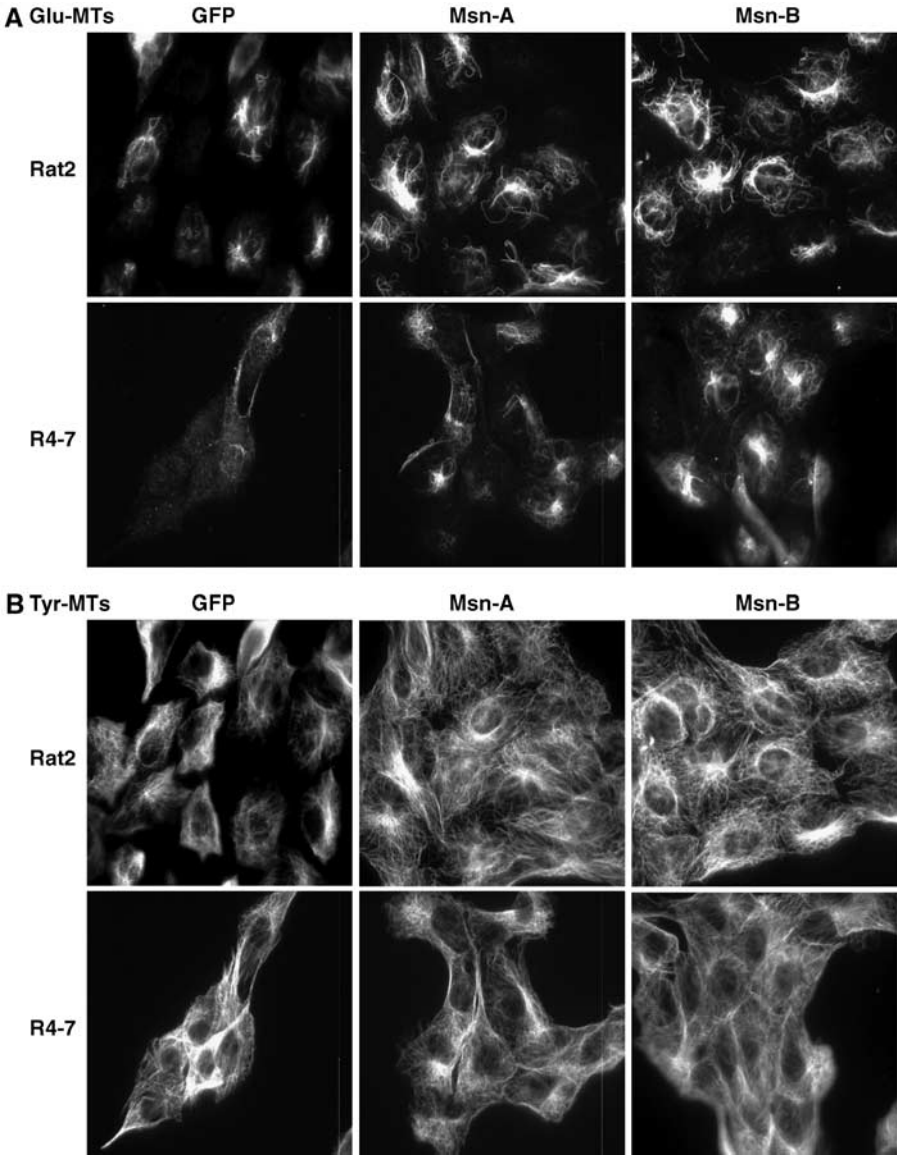

Figure 8 RNAi-mediated knockdown of moesin increases the levels of stable microtubule formation in both wt Rat2 cells and the mutant R4-7 line. (**A**) The wt Rat2 cells or mutant R4-7 cells were transfected with two independent short-interfering RNAs (indicated as Msn-A, Msn-B) on two consecutive days with equal amounts of specific RNA duplexes or a nonspecific GFP duplex. The cells were subsequently fixed and stained with a rabbit polyclonal antibody for stable Glu-MTs (A) and a rat mAb for dynamic Tyr-MTs (**B**). The cells were then incubated with fluorescently labeled secondary antibodies and images were taken as described in Materials and methods.

Discussion

These studies suggest that moesin is an important determinant of retrovirus susceptibility. Moesin is a potent antiviral protein; overexpression blocks infection by both MLV and HIV-1 reporters and infectious MLV. Knockdown of moesin by RNAi resulted in an increase in virus susceptibility, suggesting that even the endogenous basal levels of moesin in rat fibroblasts are sufficient to limit virus infection, and that moesin is an important natural determinant of cellular sensitivity to retroviral infection. The block to infection occurs at a very early stage in the viral life cycle, after viral fusion but before reverse transcription. At high multiplicity of viral infection, the block can be overcome, suggesting that it is saturable.

Moesin is a member of the closely related ezrin-radixin-moesin (ERM) family of cytoskeletal regulatory proteins that share approximately 70–80% amino-acid sequence identity (for reviews, see Bretscher, 1999; Ivetic and Ridley, 2004). Although the three proteins are very similar, the differential sensitivities of moesin and ezrin to calpain cleavage in response to Ca^{2+} signaling pathways in intact stimulated lymphocytes suggest important and specialized functions of these individual ERM proteins (Shcherbina *et al*, 1999). ERM protein expression is cell type- and organ-specific, with moesin being the most highly expressed ERM protein in human blood lymphocytes, monocytes, neutrophils and the only one detected in platelets (Schwartz-Albiez *et al*, 1995; Shcherbina *et al*, 1999). ERM proteins contain an N-terminal FERM (band four-point one, ezrin, radixin, moesin) domain, a central α-helical region and a short C-terminal domain. These proteins also share a high level of homology in their FERM domain with merlin, a tumor suppressor gene for neurofibromatosis II (Bretscher *et al*, 2002). ERM proteins

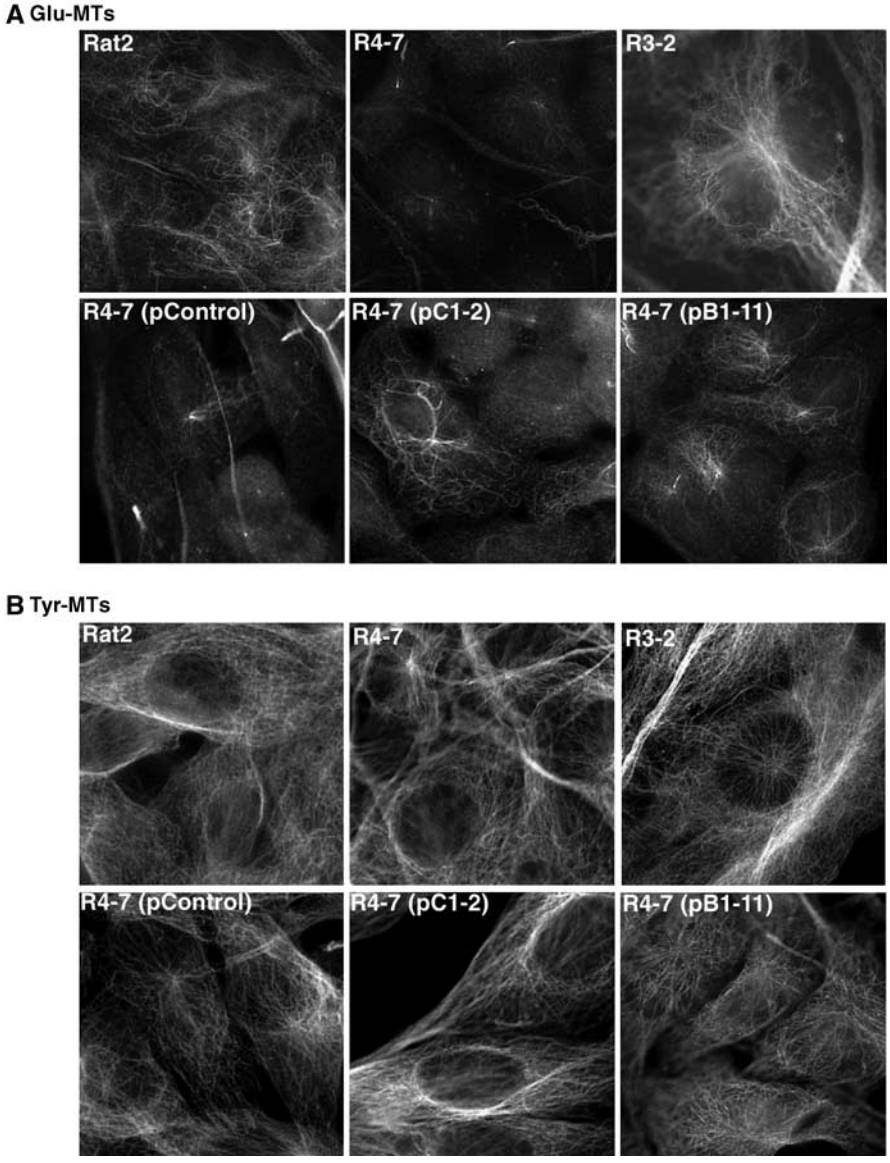

Figure 9 Virus-sensitive suppressor clones restore stable microtubule formation in R4-7 lines. Wt Rat2 cells, the virus-resistant lines R4-7 and R3-2, the empty vector R4-7 pControl line and the two R4-7 suppressor clones pC1-2 and pB1-11 were fixed and stained with a rabbit polyclonal antibody for stable Glu-MTs (**A**) and a rat mAb for dynamic Tyr-MTs (**B**). The cells were then incubated with fluorescently labeled secondary antibodies and images were taken as described in Materials and methods.

and merlin are normally inactive owing to intramolecular interactions between the amino- and carboxy-terminal domains. Phosphorylation of a conserved residue in the C-terminus in combination with acidic phospholipids can lead to activation (Bretscher, 1999). Upon activation, the highly conserved N-terminal half of ERM proteins binds to a number of integral membrane proteins, whereas the C-terminal portion directly interacts with actin filaments. Activation and inactivation of the ERM proteins can be stimulated by the Rho family of GTPases that, similar to ERM proteins, are also involved in regulating cytoskeletal dynamics in response to extracellular stimuli (Ivetic and Ridley, 2004). ERM proteins therefore act both as general crosslinkers between plasma membranes and actin filaments, as well as signal transducers in responses involving cytoskeletal remodeling.

There are indications that the cytoskeleton is involved in the early steps of infection by many viruses. Before entering the cell, a number of viruses have been shown to use the underlying actin cytoskeleton and myosin II for transport along filopodia to entry hot spots on the cell body (Lehmann *et al*, 2005). In addition, some evidence suggests that retroviruses may use the actin cytoskeleton at a post-entry step to move viral genomes from the peripheral regions of the cell, for transfer to the microtubule network where reverse transcription of viral RNA is suggested to occur (Bukrinskaya *et al*, 1998; Taunton, 2001; McDonald *et al*, 2002). An intact actin cytoskeleton or microtubule network is necessary for efficient infection of some cells by HIV-1 (Kizhatil and Albritton, 1997; Bukrinskaya *et al*, 1998; Komano *et al*, 2004). Interestingly, Nef-induced phosphorylation of the ERM-related protein merlin has recently been suggested to function in HIV-1 pathogenesis (Wei *et al*, 2005). However, the precise mechanisms and factors involved in these early post-entry events, in which the virus uses the cellular cytoskeleton to

translocate and replicate, are poorly understood. The ability of moesin to act as a general crosslinker between plasma membranes and actin filaments, as well as its function in cytoskeletal remodeling, suggests that it may be an important regulator of such events. Indeed, a number of other cytoskeletal regulatory proteins have been shown to play a role in virus replication. IQGAP1 (Leung *et al*, 2006), an actin- and microtubule-interacting protein, and Kif4 (Kim *et al*, 1998; Tang *et al*, 1999), a microtubule-associated motor protein, both bind to the matrix protein of MLV and play positive roles in viral replication. In addition, overexpression of FEZ-1, a microtubule-associated neuronal transport protein interacting with kinesin (Gindhart *et al*, 2003), blocks the transport of retroviral DNA into the nucleus after reverse transcription (Naghavi *et al*, 2005).

Overexpression of moesin may have many downstream effects on cellular physiology that could mediate the viral block. Indeed, our findings suggest that moesin negatively regulates the stable microtubule network within the host cell, and that this network is important in early post-entry events in infection. The block to virus infection is very similar to that seen in the R4-7 cell line, a mutant Rat2 line selected for virus resistance after heavy chemical mutagenesis (Gao and Goff, 1999). Remarkably, the R4-7 line is also devoid of stable microtubules. The moesin gene does not appear to be modified or overexpressed in the virus-resistant R4-7 cells, suggesting that mutations of another unknown gene(s) are responsible for the resistance (Gao and Goff, 1999). Therefore, two independent selections for virus resistance have resulted in the loss of stable microtubules and in the same virus-resistant phenotype, strongly suggesting that the potent block to virus infection observed in both these lines can be attributed to these cytoskeletal defects. Notably, both stable microtubules (Cook *et al*, 1998; Palazzo *et al*, 2001) and moesin (Ivetic and Ridley, 2004) are known to be regulated by the Rho-GTPase pathway, and therefore gene(s) involved in this pathway may have been affected in the R4-7 line. Finally, if the loss of stable microtubules was truly responsible for the virus resistance of R4-7, then the isolation of virus-sensitive revertants should be accompanied by the restoration of stable microtubules. This expectation was indeed met. Two lines selected for virus sensitivity (Gao and Goff, 2004) were both found to have recovered wt levels of stable microtubules. Similarly, the defect in stable microtubule formation was reversed and virus sensitivity was restored to a moesin-overexpressing line upon excision of moesin cDNA from the genome, suggesting that loss of Glu-MTs was the cause of viral resistance in this line. The fact that multiple revertant clones restored stable microtubules strongly suggests that these structures play an important role in infection.

Both full-length and the N-terminal domain of moesin, with or without fusion to the zeocin selectable marker, impose a potent block to infection. The N-terminal domain of moesin, which is sufficient to confer resistance to retroviral infection, contains a FERM domain. These domains function frequently as binding sites that link cytoskeletal proteins to integral membrane proteins (Chishti *et al*, 1998). Notably, this domain is also present in a large group of unconventional myosins such as myosin-X (Myo 10) and can act as a link to integrins and microtubules (Zhang *et al*, 2004). The FERM domain of moesin may therefore interact with microtubules, and it is tempting to speculate that moesin may be capable of regulating or interfering with the transition of viral genomes from the actin cytoskeleton to the microtubule network by controlling stable microtubule formation. Stable microtubules have been suggested to function as specialized tracks for vesicle and cytoskeletal trafficking (Wen *et al*, 2004), further supporting the idea that moesin is involved in mislocalization of internalized virus particles. Indeed, an involvement of ezrin and moesin in actin assembly has been proposed to facilitate aggregation of phagosome/endosomes (Defacque *et al*, 2000). This hypothesis was recently supported by the finding that a dominant-negative N-terminal moesin fragment delayed the maturation rates of phagosomes, most likely because of impaired actin assembly (Erwig *et al*, 2006). It is also tempting to suggest that reverse transcription of viral RNA, thought to occur on microtubules (Bukrinskaya *et al*, 1998; McDonald *et al*, 2002), may actually occur on the stable microtubule subset. This would explain the findings that moesin, which disrupts stable microtubules, inhibits retroviral replication before reverse transcription. In the absence of stable microtubules, reverse transcription complexes may be unable to form or function. Further studies on the function of moesin may provide invaluable insights into the poorly understood post-entry event known as 'uncoating' and the role of the host cytoskeleton therein, and may also allow novel control over cell susceptibility to infection.

Materials and methods

cDNA library screen for retrovirus-resistant cells

The R4-7 cDNA library was constructed as described (Gao *et al*, 2002). After introduction of a *Sal*I site in the pBabe-HAZ retroviral vector (Gao *et al*, 2002), the cDNAs were inserted between *Sal*I and *Not*I sites. A library of transducing viruses was then generated by cotransfection of 293T cells with a mixture of the pBabe-HAZ cDNA library, the HIV-1 gag–pol-expressing plasmid (p8.91) (Naldini *et al*, 1996) and the VSV-G envelope-expressing plasmid (pMD.G) (Naldini *et al*, 1996), as described in Gao *et al* (2002). The culture supernatants collected at 48, 72 and 96 h were further used to infect Rat2 cells and the transduced clones expressing the cDNA were isolated by selection in zeocin (50 μg/ml).

Viruses and producer cell line

MLV-N-neo MLV-B-neo, MoMLV-puro and HIV-1-puro viruses pseudotyped with VSV-G envelope (Naldini *et al*, 1996) were produced by transfection of 293T cells using a combination of three expression vectors, as described in Naghavi *et al* (2005). HIV-1-puro virus carrying an amphotropic envelope was generated by replacing pMDG (Naldini *et al*, 1996) with the pHit456 (Yap *et al*, 2000) vector in the previously described protocol (Naghavi *et al*, 2005). The same protocol was used for preparation of VSV-G-pseudotyped (Naldini *et al*, 1996) HIV-1-TK viral vectors using the TK-expressing plasmid, TRIP-TK, generated by replacing GFP in TRIP-GFP (Zennou *et al*, 2001) with the TK gene (a kind gift from Dr Guangxia Gao, Chinese Academy of Sciences, Beijing, China) and the gag–pol-expressing vector p8.91 (Naldini *et al*, 1996). MLV-GFP virus was recovered from the producer line ECO-Phoenix-MLV (Gao and Goff, 1999).

Infection of cultured cells and transduction assays

Target cells (1×10^5) were infected as described in Naghavi *et al* (2005). Polybrene was added to infections at a final concentration of 8 μg/ml. MLV-GFP titration was assayed by flow cytometry 24 h after infection. HIV-1-puro, MoMLV-puro or MLV-neo, titers were measured by infection of Rat2 or 293A cells and colony counting after selection in puromycin (1.5 μg/ml) or G418 (500 μg/ml for Rat2 cells and 850 μg/ml for 293A cells), respectively.

Quantitative real-time PCR

Cytoplasmic RNA was converted into double stranded (ds) cDNA and used as template in QRT-PCR using SYBR Green JumpStart Taq ReadyMix (Sigma) as described in Naghavi *et al* (2005) and primers outlined in Supplementary Table S2. Total and transgene moesin transcript levels were determined using primers specific to moesin sequences (primers 1 and 9) or a combination of one moesin-specific primer together with primers specific to vector sequences flanking the moesin cloning site (primers 7 and 8 or 6 and 9), respectively. The number of target copies in each sample was interpolated from its detection threshold (C_T) value using a GAPDH plasmid standard curve as described (in Naghavi *et al,* 2005).

Generation of cells stably expressing moesin variants

Zeocin-fused moesin variants were amplified and subcloned into pcDNA3.1$^+$ vectors (Invitrogen) using the following primers (Supplementary Table S2), full-length moesin (primers 1 and 3) or C-terminally truncated moesin (primers 1 and 5). A total of 50–70% confluent Rat2 or 293A cells were then transfected with 4 μg of the moesin constructs or the control empty pcDNA3.1$^+$ vector as described (in Naghavi *et al,* 2005). At 48 h after transfection, cells were selected in G418 (500 μg/ml for Rat2 cells and 850 μg/ml for 293A) and several resistant clones of each stable line were further tested in transduction assays.

Immunoblotting

Whole-cell lysates from the Rat2 or the 293A stable lines overexpressing full-length or truncated zeocin-tagged moesin were fractionated by SDS–polyacrylamide gel electrophoresis (PAGE), transferred to nitrocellulose membrane and probed with the indicated antisera, anti-Sh-ble (zeocin) (CAYLA, cat no. ANT-SH), anti-β-actin (Sigma, cat no. A5316) or anti-GAPDH (Santa Cruz, cat no. SC25778).

Reverse transcriptase assay

To examine virus viability, 293T cells were transiently transfected with the Moloney proviral DNA (pNCS). Virus was harvested and 10-fold serial dilutions (10 ×, 100 ×, 1000 ×) were used to infect naïve Rat2 cells or the stably expressing zeocin-tagged full-length or C-terminally truncated moesin lines. Culture supernatants were collected on successive days and monitored for virus production by RT assay.

RNA interference

wt or mutant R4-7 cells were transfected with two independent pre-designed siRNAs (Ambion) or a nonspecific control siRNA duplex targeted to GFP using Oligofectamine transfection reagent (Invitrogen) as described (in Naghavi *et al,* 2005). Cells were transfected on two consecutive days with 300 pmol of each of the RNA duplexes and subsequently seeded, infected with various amounts of MoMLV-puro or HIV-1-puro and selected as described above. Levels of endogenous moesin expression in Rat2 cells transfected with nonspecific (GFP) or moesin-specific siRNA duplexes were measured by quantitative RT–PCR, as described above.

Quantitative real-time PCR of viral DNA

Target cells were infected with ecotropic MLV-GFP, as described (in Naghavi *et al,* 2005). Hirt DNA was isolated at 24 h after infection according to the standard protocol (Arad, 1998). One microliter of Hirt DNA was used as template for QRT-PCR using SYBR Green JumpStart *Taq* ReadyMix (Sigma). Primers to amplify GFP sequence (GFP-FP and GFP-RP), the MLV minus-strand strong stop DNA (MSS-FP and MSS-RP), the plus-strand (PS-FP and PS-RP) viral DNA and the MLV LTR–LTR junction, (MR5784 and MR4091) (Smith *et al*, 1997) have been previously reported (Gao and Goff, 1999).

Trafficking of transferrin in Rat2 and R4-7 cells

Cells grown on gelatin-coated coverslips were incubated with 0.1 mg/ml human transferrin conjugated to tetramethylrhodamine (Molecular Probes) at 4°C for 1 h. Cells were washed three times with cold PBS (to remove unbound transferrin), and warm medium was added and the cells were shifted to 37°C and fixed with 3% parafolmadehyde at various time points thereafter. For immunofluorescence staining, the cells were permeabilized with 0.1% Triton X-100 and incubated with an antibody against tubulin (DM1A, Sigma), followed by an FITC-conjugated antimouse secondary from Jackson ImmunoResearch Laboratories (West Grove, PA). Images were taken as described below.

Quantification of transferrin uptake in Rat2, R4-7 and the moesin-overexpressing lines

Target cells (10^5 cells/well) were seeded in 24-well plates, and 24 h later cells were serum-starved for 30 min in growth media containing 0.1% BSA. Biotin-labeled transferrin 250 ng/ml (Molecular Probes) was added and cultures were incubated on ice for 1 h. Unbound ligand was removed with several quick washes with pre-warmed serum-free media. Bound transferrin was allowed to internalize upon incubation in 0.1% BSA-containing medium for various lengths of time at 37°C (2, 5 and 8 min to avoid any recycling). Non-internalized, membrane-bound transferrin was removed by a 2 min incubation with 0.5 M NaCl, 0.2 M sodium acetate buffer, pH 4.5, followed by several wash cycles with the same solution. Internalized biotinylated transferrin was quantitated by Western blotting using 0.5 μg/ml NeutraAvidin conjugated to horseradish peroxidase (Molecular Probes).

Immunofluorescence microscopy

Cells grown on acid-washed coverslips were fixed either in parafolmadehyde or −20°C methanol for 5–10 min and rehydrated in TBS. They were stained for 1 h with a rabbit polyclonal antibody SG (1:400; Gundersen *et al*, 1984) for stable Glu-MTs and a rat mAb YL1/2 (1:10; European Collection of Animal Cell Cultures, Salisbury, UK) for dynamic Tyr-MTs. Fluorescence labeled secondary antibodies that were pre-absorbed to eliminate cross-species reactivity were from Jackson ImmunoResearch Laboratories (West Grove, PA). All stainings were performed in TBS with 10% normal goat serum. For fluorescence microscopy, cells were observed with a Nikon Optiphot microscope and images were captured with a MicroMax cooled CCD camera (Princeton Instruments) using the Metamorph software (Universal Imaging).

Supplementary data

Supplementary data are available at *The EMBO Journal* Online (http://www.embojournal.org).

Acknowledgements

This work was supported by the PHS grants CA30488 to SPG, and GM068595 to GGG, R37CA30488 from the National Cancer Institute. We thank Dr Warner Greene at the Gladstone Institute of Virology and Immunology, University of California, San Francisco for kindly providing us with the Vpr-BlaM expression vector; Dr Guangxia Gao at the Institute of Microbiology, Chinese Academy of Sciences, Beijing, China for reagents and advice and Dr Greg Towers at the Wohl Virion Centre, Department of Immunology and Molecular Pathology, University College London, London, UK, for providing us with retroviral vectors. We are grateful to Dr Derek Walsh at the Department of Microbiology at NYU for critically reading the manuscript. MHN was supported with a postdoctoral scholarship from The Swedish Foundation for International Cooperation in Research and Higher Education. MHN is an Associate and SPG is an investigator at the Howard Hughes Medical Institute.

References

Arad U (1998) Modified Hirt procedure for rapid purification of extrachromosomal DNA from mammalian cells. *Biotechniques* **24:** 760–762

Bick MJ, Carroll JW, Gao G, Goff SP, Rice CM, MacDonald MR (2003) Expression of the zinc-finger antiviral protein inhibits alphavirus replication. *J Virol* **77:** 11555–11562

Bretscher A (1999) Regulation of cortical structure by the ezrin–radixin–moesin protein family. *Curr Opin Cell Biol* **11:** 109–116

Bretscher A, Edwards K, Fehon RG (2002) ERM proteins and merlin: integrators at the cell cortex. *Nat Rev Mol Cell Biol* **3:** 586–599

Bukrinskaya A, Brichacek B, Mann A, Stevenson M (1998) Establishment of a functional human immunodeficiency virus

type 1 (HIV-1) reverse transcription complex involves the cytoskeleton. *J Exp Med* **188:** 2113–2125

Cavrois M, De Noronha C, Greene WC (2002) A sensitive and specific enzyme-based assay detecting HIV-1 virion fusion in primary T lymphocytes. *Nat Biotechnol* **20:** 1151–1154

Chishti AH, Kim AC, Marfatia SM, Lutchman M, Hanspal M, Jindal H, Liu SC, Low PS, Rouleau GA, Mohandas N, Chasis JA, Conboy JG, Gascard P, Takakuwa Y, Huang SC, Benz Jr EJ, Bretscher A, Fehon RG, Gusella JF, Ramesh V, Solomon F, Marchesi VT, Tsukita S, Arpin M, Louvard D, Tonks NK, Anderson JM, Fanning AS, Bryant PJ, Woods DF, Hoover KB (1998) The FERM domain: a unique module involved in the linkage of cytoplasmic proteins to the membrane. *Trends Biochem Sci* **23:** 281–282

Cook TA, Nagasaki T, Gundersen GG (1998) Rho guanosine triphosphatase mediates the selective stabilization of microtubules induced by lysophosphatidic acid. *J Cell Biol* **141:** 175–185

Defacque H, Egeberg M, Habermann A, Diakonova M, Roy C, Mangeat P, Voelter W, Marriott G, Pfannstiel J, Faulstich H, Griffiths G (2000) Involvement of ezrin/moesin in *de novo* actin assembly on phagosomal membranes. *EMBO J* **19:** 199–212

Erwig LP, McPhilips KA, Wynes MW, Ivetic A, Ridley AJ, Henson PM (2006) Differential regulation of phagosome maturation in macrophages and dendritic cells mediated by Rho GTPases and ezrin–radixin–moesin (ERM) proteins. *Proc Natl Acad Sci USA* **103:** 12825–12830

Gao G, Goff SP (1999) Somatic cell mutants resistant to retrovirus replication: intracellular blocks during the early stages of infection. *Mol Biol Cell* **10:** 1705–1717

Gao G, Goff SP (2004) Isolation of suppressor genes that restore retrovirus susceptibility to a virus-resistant cell line. *Retrovirology* **1:** 30

Gao G, Guo X, Goff SP (2002) Inhibition of retroviral RNA production by ZAP, a CCCH-type zinc finger protein. *Science* **297:** 1703–1706

Garrus JE, von Schwedler UK, Pornillos OW, Morham SG, Zavitz KH, Wang HE, Wettstein DA, Stray KM, Cote M, Rich RL, Myszka DG, Sundquist WI (2001) Tsg101 and the vacuolar protein sorting pathway are essential for HIV-1 budding. *Cell* **107:** 55–65

Gindhart JG, Chen J, Faulkner M, Gandhi R, Doerner K, Wisniewski T, Nandlestadt A (2003) The kinesin-associated protein UNC-76 is required for axonal transport in the Drosophila nervous system. *Mol Biol Cell* **14:** 3356–3365

Gundersen GG, Kalnoski MH, Bulinski JC (1984) Distinct populations of microtubules: tyrosinated and nontyrosinated alpha tubulin are distributed differently *in vivo*. *Cell* **38:** 779–789

Hinrichsen L, Harborth J, Andrees L, Weber K, Ungewickell EJ (2003) Effect of clathrin heavy chain- and alpha-adaptin-specific small inhibitory RNAs on endocytic accessory proteins and receptor trafficking in HeLa cells. *J Biol Chem* **278:** 45160–45170

Ivetic A, Ridley AJ (2004) Ezrin/radixin/moesin proteins and Rho GTPase signalling in leucocytes. *Immunology* **112:** 165–176

Kikonyogo A, Bouamr F, Vana ML, Xiang Y, Aiyar A, Carter C, Leis J (2001) Proteins related to the Nedd4 family of ubiquitin protein ligases interact with the L domain of Rous sarcoma virus and are required for gag budding from cells. *Proc Natl Acad Sci USA* **98:** 11199–11204

Kim W, Tang Y, Okada Y, Torrey TA, Chattopadhyay SK, Pfleiderer M, Falkner FG, Dorner F, Choi W, Hirokawa N, Morse III HC (1998) Binding of murine leukemia virus Gag polyproteins to KIF4, a microtubule-based motor protein. *J Virol* **72:** 6898–6901

Kizhatil K, Albritton LM (1997) Requirements for different components of the host cell cytoskeleton distinguish ecotropic murine leukemia virus entry via endocytosis from entry via surface fusion. *J Virol* **71:** 7145–7156

Komano J, Miyauchi K, Matsuda Z, Yamamoto N (2004) Inhibiting the Arp2/3 complex limits infection of both intracellular mature vaccinia virus and primate lentiviruses. *Mol Biol Cell* **15:** 5197–5207

Lehmann MJ, Sherer NM, Marks CB, Pypaert M, Mothes W (2005) Actin- and myosin-driven movement of viruses along filopodia precedes their entry into cells. *J Cell Biol* **170:** 317–325

Leung J, Yueh A, Appah FS, Yuan B, de Los Santos K, Goff SP (2006) Interaction of Moloney murine leukemia virus matrix protein with IQGAP. *EMBO J* **25:** 2155–2166

Lin SX, Gundersen GG, Maxfield FR (2002) Export from pericentriolar endocytic recycling compartment to cell surface depends on stable, detyrosinated (glu) microtubules and kinesin. *Mol Biol Cell* **13:** 96–109

McDonald D, Vodicka MA, Lucero G, Svitkina TM, Borisy GG, Emerman M, Hope TJ (2002) Visualization of the intracellular behavior of HIV in living cells. *J Cell Biol* **159:** 441–452

Naghavi MH, Hatziioannou T, Gao G, Goff SP (2005) Overexpression of fasciculation and elongation protein zeta-1 (FEZ1) induces a post-entry block to retroviruses in cultured cells. *Genes Dev* **19:** 1105–1115

Naldini L, Blomer U, Gallay P, Ory D, Mulligan R, Gage FH, Verma IM, Trono D (1996) *In vivo* gene delivery and stable transduction of nondividing cells by a lentiviral vector. *Science* **272:** 263–267

Palazzo AF, Cook TA, Alberts AS, Gundersen GG (2001) mDia mediates Rho-regulated formation and orientation of stable microtubules. *Nat Cell Biol* **3:** 723–729

Schwartz-Albiez R, Merling A, Spring H, Moller P, Koretz K (1995) Differential expression of the microspike-associated protein moesin in human tissues. *Eur J Cell Biol* **67:** 189–198

Shcherbina A, Bretscher A, Kenney DM, Remold-O'Donnell E (1999) Moesin, the major ERM protein of lymphocytes and platelets, differs from ezrin in its insensitivity to calpain. *FEBS Lett* **443:** 31–36

Smith CM, Potts III WB, Smith JS, Roth MJ (1997) RNase H cleavage of tRNAPro mediated by M-MuLV and HIV-1 reverse transcriptases. *Virology* **229:** 437–446

Stremlau M, Owens CM, Perron MJ, Kiessling M, Autissier P, Sodroski J (2004) The cytoplasmic body component TRIM5alpha restricts HIV-1 infection in Old World monkeys. *Nature* **427:** 848–853

Tang Y, Winkler U, Freed EO, Torrey TA, Kim W, Li H, Goff SP, Morse III HC (1999) Cellular motor protein KIF-4 associates with retroviral Gag. *J Virol* **73:** 10508–10513

Taunton J (2001) Actin filament nucleation by endosomes, lysosomes and secretory vesicles. *Curr Opin Cell Biol* **13:** 85–91

von Schwedler UK, Stuchell M, Muller B, Ward DM, Chung HY, Morita E, Wang HE, Davis T, He GP, Cimbora DM, Scott A, Krausslich HG, Kaplan J, Morham SG, Sundquist WI (2003) The protein network of HIV budding. *Cell* **114:** 701–713

Wei BL, Arora VK, Raney A, Kuo LS, Xiao GH, O'Neill E, Testa JR, Foster JL, Garcia JV (2005) Activation of p21-activated kinase 2 by human immunodeficiency virus type 1 Nef induces merlin phosphorylation. *J Virol* **79:** 14976–14980

Wen Y, Eng CH, Schmoranzer J, Cabrera-Poch N, Morris EJ, Chen M, Wallar BJ, Alberts AS, Gundersen GG (2004) EB1 and APC bind to mDia to stabilize microtubules downstream of Rho and promote cell migration. *Nat Cell Biol* **6:** 820–830

Westermann S, Weber K (2003) Post-translational modifications regulate microtubule function. *Nat Rev Mol Cell Biol* **4:** 938–947

Yap MW, Kingsman SM, Kingsman AJ (2000) Effects of stoichiometry of retroviral components on virus production. *J Gen Virol* **81:** 2195–2202

Yasuda J, Hunter E, Nakao M, Shida H (2002) Functional involvement of a novel Nedd4-like ubiquitin ligase on retrovirus budding. *EMBO Rep* **3:** 636–640

Zennou V, Serguera C, Sarkis C, Colin P, Perret E, Mallet J, Charneau P (2001) The HIV-1 DNA flap stimulates HIV vector-mediated cell transduction in the brain. *Nat Biotechnol* **19:** 446–450

Zhang H, Berg JS, Li Z, Wang Y, Lang P, Sousa AD, Bhaskar A, Cheney RE, Stromblad S (2004) Myosin-X provides a motor-based link between integrins and the cytoskeleton. *Nat Cell Biol* **6:** 523–531

